Received September 8, 2014, accepted November 3, 2014, date of publication November 20, 2014,
date of current version December 5, 2014.

Digital Object Identifier 10.1109/ACCESS.2014.2369506

Think Small: Nanopores for Sensing and Synthesis

WINSTON TIMP[1], (Member, IEEE), ALLISON M. NICE[1], EDWARD M. NELSON[2], VOLKER KURZ[2], KIM McKELVEY[2], AND GREGORY TIMP[3], (Fellow, IEEE)

[1]Department of Biomedical Engineering, Johns Hopkins University, Baltimore, MD 21218, USA
[2]Department of Electrical Engineering, University of Notre Dame, Notre Dame, IN 46556, USA
[3]Department of Electrical Engineering and Department of the Biological Science, University of Notre Dame, Notre Dame, IN 46556, USA

Corresponding author: G. Timp (gtimp@nd.edu)

This work was supported in part by the National Science Foundation under Grant CCF 1129098 and Grant DBI 1256052, in part by the National Institutes of Health-Small Business Innovation Research Phase II under Grant 5R44EB008589-04a, and in part by the Keough-Hesburgh Professorship. Disclosure: W. Timp and G. Timp have patents under license by Oxford Nanopore Technology.

ABSTRACT It is now possible to manipulate individual molecules using a nanopore to read DNA and proteins, or write DNA by inserting mini-genes into cells. Furthermore, development of these methodologies will kick open the door to new biology and chemistry that has been logistically intractable previously. Nanopore technology will place molecular and sub-molecular analysis within the reach of the typical bench-top scientist or clinical lab—no longer limited to genomics or mass spectrometry specialists. Moreover, the prospects for synthetic biology—using nanopores to program or reprogram cells–are promising as well, but have been examined only at the level of a single cell, so far.

INDEX TERMS Nanopore, single molecule force spectroscopy, AFM, DNA sequencing, scanning ion conductance microscopy, single cell transfection.

I. INTRODUCTION

A nanometer-diameter pore in a nanometer-thick membrane immersed in electrolyte works like a miniaturized Coulter counter [1]. Charged, single molecules are forced through the pore by an electric field and detected by changes in the electrolytic pore current. (The supplemental video S1 is a confocal image of a cross-section through a nanopore in a silicon nitride membrane showing fluorescent DNA plasmids translocating through the pore.) The molecular component trapped in the pore presents an energy barrier to the passage of ions that affects the current in a distinctive way. To characterize molecules with sub-molecular sensitivity, stringent sub-nanometer control is required over both the molecular configuration in the pore and the translocation kinetics. This precision translates directly into control of the distribution of the electric field in the pore. While there is a precedent for this kind of precision—the single electron transistor is the most sensitive device for charge measurement ever made [2]—it is difficult to achieve this control under physiological conditions in electrolyte where the Debye length can be comparable to the molecular charge density.

Church *et al.* [3] first suggested that polymers could be characterized by measuring the altered current as (sub-molecular) monomers pass through the pore. Kasianowicz *et al.* [4] subsequently tested this idea by characterizing DNA and RNA in α-hemolysin (α-HL) nanopores using techniques developed in electrophysiology for ion-channel measurements. Proteins such as α-HL, MspA and their variants, embedded in a phospholipid layer offer exquisitely precise self-assembled biological nanopores and have demonstrated a facility for discriminating individual nucleotides in DNA. However, modifying or designing pore structures from scratch to accommodate anything besides nucleic acids is a challenging endeavor; *ab initio* protein design is still beyond the pale [5]. On the other hand, relying on relatively facile silicon nanofabrication, nanopores sputtered through solid-state membranes represent an appealing alternative; although the structure is less precise than a self-assembled biological pore, sub-nanometer precision is possible, but not routine.

For the last 20 years, the Coulter principle has been explored assiduously; that progress has been reviewed elsewhere [6]–[8]. Nanopores are now finally poised to kick open the door to applications in **1.** medicine (DNA sequencing and protein sequencing), **2.** threat detection (sniffing out single molecules of protein, polymers or explosives), **3.** deep-tissue, high-resolution molecular imaging (nanoscopy) and

4. synthetic biology (cell transfection). However, they are still plagued by nagging problems that curb their commercial viability such as deficient chemical specificity, stringent manufacturing requirements; parasitics that adversely affects the response time; pore clogging; and onerous electrical parasitics. Here, we review the status of nanopore technology to provide an up-to-the-minute assessment of some of the prospects for the applications in sensing and synthesis, delineate the performance limitations and deficiencies, and sketch out how to fix them.

II. DISCUSSION

A. SEQUENCING DNA

So far, the main application driving the development of nanopore sensing has been sequencing DNA. Nanopore sequencing offers kilo-base long reads from a single molecule, offering a leg-up on 21st century genomics, e.g. easier *de novo* assembly [9]–[11]. However, single nucleotide resolution requires stringent sub-nanometer control over both the DNA configuration in the pore and the translocation kinetics because the equilibrium distance between nucleotides is only 0.35 nm. The molecular component trapped in the pore might be discriminated by the occluded volume (e.g. purines are larger than pyrimidines), their mobility or their charge [12]. However, the differences in the electrical signal between bases are typically only a few pico-Amperes and require signal averaging against a noisy background of at least 2 pA-rms associated with the pore resistance. Different methods of controlling the translocation kinetics have been pursued: from changing the temperature [13] and viscosity of the electrolyte [14] to using proteins (polymerases, helicases) [15], [16] to advance the molecule slowly. Other methodologies involve stretching DNA in a pore smaller than its hydrodynamic diameter [17] or embedding electrodes for control using time-varying electric fields [18].

The forces associated with a translocation through a nanopore in a solid-state membrane and the concomitant changes in the electrolytic current have been measured directly by tethering a single-stranded DNA (ssDNA) molecule to the tip of an atomic force microscope (AFM) cantilever (Fig. 1a) [19]. The measurements were accomplished using solid-state nanopores with a bi-conical topography and a diameter as small as 1.0 nm, comparable to the DNA, in silicon nitride membranes 6–10 nm thick [20]. Early work exploring the forces and current affecting double stranded DNA (dsDNA) [21], [22] or carbon nanotubes (CNT) [23] in synthetic nanopores either focused on pore diameters ($>$6 nm) that were too large compared to the diameter of DNA to produce an adequate signal for sequencing or required voltages that were too small ($\sim$100 mV) to suppress translational noise [7].

These measurements revealed two types of translocation kinetics: ''slip-stick'' motions (Fig. 1b) and frictionless sliding (Fig. 1c). The force plateaus associated with the molecule sliding frictionlessly through the pore may provide an opportunity for sequencing since regular patterns were observed intermittently in the force and corresponding current, separated by 0.3–0.72 nm in both homopolymers and heteropolymers, which were consistent with the spacing between partially stretched nucleotides (Fig. 1d). From the perspective of sequencing, an analytical tool with long read lengths that can count repetitive segments would be invaluable as it becomes exponentially harder to assemble a genome as the number of repeats grows [9]–[11]. To test the prospects for detecting repeats, a subset of data obtained on a force plateau when a single heteropolymer poly(C_4A_4)$_{20}$ slid through a pore (Fig. 1d) was identified and the fluctuations there were analyzed. It was reasoned that the difference in size between a purine (A) and pyrimidine (C), and nucleobase mobility differential [12] would facilitate discrimination.

Figure 1d shows a typical result acquired when a single molecule was extracted from a 1.4×1.6 nm^2 cross-section pore against a potential of 0.4 V. Associated with a force plateau (Fig. 1c), a blockade was observed that was consistent with a single ssDNA molecule occluding the pore. An analysis of the fluctuations in the blockade revealed regular fluctuations with a mean lag of 0.30 ± 0.01 nm in the current that were modulated. The current autocorrelation function (ACF) displayed a maximum near 2.3 nm, which was consistent with the chemical constituency of the heteropolymer: *i.e.* for C_4A_4 0.3 nm $\times$ 4 $\times$ 2 $=$ 2.4 nm. Whereas the fluctuations viewed through the ACFs are emblematic of a heteropolymer, the force and current differences between A and C are minute ($<$1 pN and $<$20 pA, respectively) and difficult to identify without improvements in the post acquisition signal recovery [24], [25]. To improve the conditions of the test, the pore topography should be modified to tighten the electric field distribution in the pore as it extends over a few nanometers due to a combination of effects associated with the membrane thickness and the cone angle defining the bi-conical pore. Thus, multiple monomers, or base-pairs (in the case of DNA) likely influence the current signature at the same time [26].

There are several workarounds to the problems with chemical specificity and single nucleotide resolution. First, the membrane could be made thinner using a molecular sheet fashioned from graphene [27] or even more exotic materials, such as MoS_2 [28]. However, simulations indicate that the graphene thickness will only support two different conductance states—it is too thin to distinguish all the bases—whereas MoS_2 may show four states [28]. Moreover, bases stick to hydrophobic graphene during a translocation and clog the pore, [29] but not necessarily to hydrophilic MoS_2 [28]. On the other hand, purposefully functionalizing a pore with recognition reagents that bind nucleobases may offer some relief; [30] this prospect has been reviewed elsewhere [31].

We propose that multiple monomers affecting the blockade current are not really the problem so long as the translocation rate is stringently controlled [25]. Consider the situation where three DNA base pairs, a triplet, affect the pore

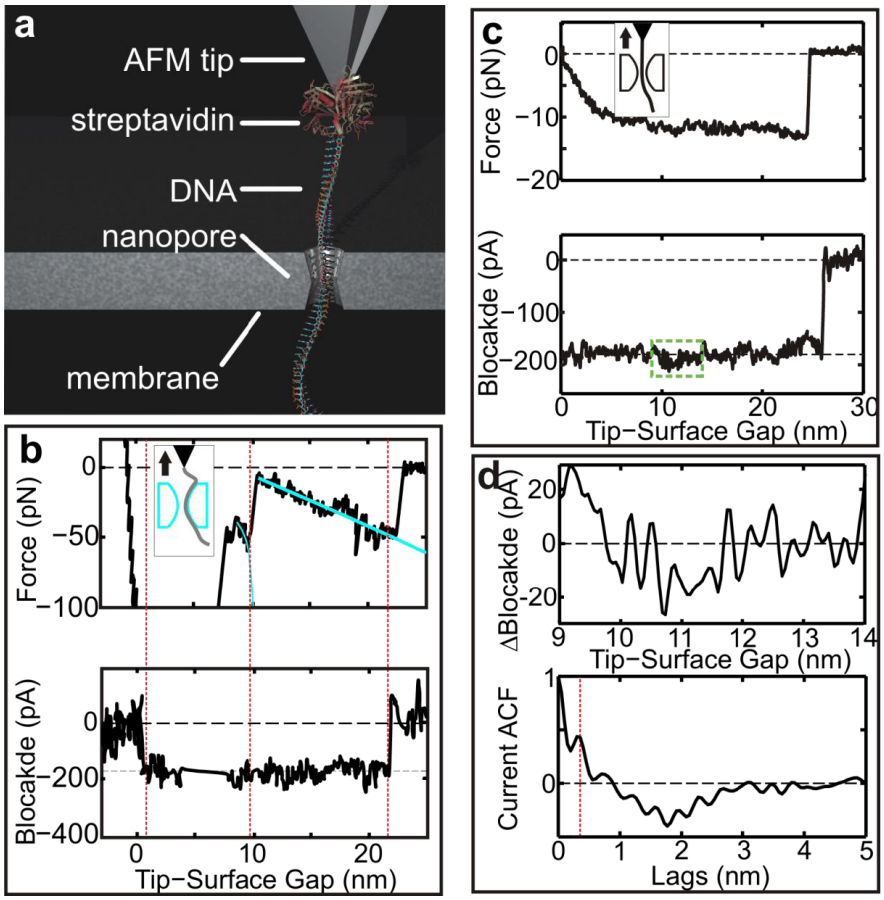

FIGURE 1. **Direct simultaneous measurements of the current and force on ssDNA in a solid-state nanopore. (a) Cutaway schematic showing biotinylated ssDNA (btssDNA), tethered to the AFM tip through a bond to streptavidin, translocating through the nanopore. (b) The force (top) and current blockade (bottom) measured during a "stick-slip" translocation under an applied potential of 0.5 V while the AFM cantilever with poly(T)$_{150}$ tethered to it was retracted from a 2.1 nm diameter pore, showing a typical loading of a single molecule that produces a force-extension curve reflecting the molecular elasticity. The red lines demarcate when the molecule enters the pore and the rupture of a sticking bond allowing the molecule to exit. The blue lines represent fits to the freely-jointed chain model for each individual stretch. The cartoon inset shows the assumed molecular configuration at the first rupture event and the direction of the cantilever motion. (c) Like (b), the force (top) and blockade current (bottom) measured during the "frictionless" translocation of poly(C_4A_4)$_{20}$ as it is extracted from a 1.4 × 1.6 nm^2 cross-section pore against an applied potential of 0.4 V. The green box highlights a 5 nm portion of the current data from which the ACF was calculated. The cartoon shows the assumed molecular configuration with the arrow indicating the direction of the cantilever motion. (d) A magnified view showing the change in blockade current (top) in the 5 nm window and the corresponding ACF (bottom) of the blockade current of the same data. Adapted from reference [19].**

current—this gives 64 possible combinations, 64 different current levels. These current levels are not always easily distinguishable from each other (Fig. 2a) by themselves due to the inherent signal-to-noise. For example, GTG can be easily distinguished from other triplets, but TCG is hard to distinguish from its neighbors based on current alone. However, as the bases advance through the pore, with a state change the next base (assuming completely random distribution of bases) has an equal probability of A, C, G, or T, *i.e.* in the case of TCG the next triplet is CGA, CGC, CGG, or CGT. This can be represented using a hidden Markov model (HMM) with a chain of hidden states (bases) only observable indirectly (via the current). For a HMM, a state diagram can be constructed from output probabilities, the probability distribution of currents observed for each state, and transition probabilities, in this case 25% for each of A, C, G, and T. It is then possible to maximize the joint probability, using the entire chain of observed currents to determine the hidden state chain. Joint probability is given by $P(I\,(t)|\,k) \times T_{jk}$ where $P(I\,(t)|\,k)$ is the output probability for state k, and T_{jk} the transition probability between states j and k. The total joint probability is given by $\delta_k \prod_t P(I\,(t)|\,k_t) \times T_{(t-1)(t)}$ where $\delta_k$is the probability that each of the states is initially occupied. A Viterbi algorithm determines at each step the most probable combination of previous steps to reach that point, given by: $V_k\,(t) = P(I\,(t)|\,k)\max_j\,(V_j(t-1) \times T_{jk})$.

Using this method the sequence of (in this case triplet) states can be determined that delineate the DNA sequence. This method can be used on any polymer, just with an expanded number of possible states depending on the number of monomers influencing the current. However, this model does depend on having the polymer advance one (and only one) monomer at a time through the pore. If not, the transition probability matrix has to be expanded to include the probability of staying in the same state, or advancing two monomers, though this may dramatically increase the state-space. The model can best be trained empirically to determine both output probabilities and the transition matrix.

Despite vexing problems with chemical specificity and control of the translocation, biological nanopores have been used to sequence DNA, and the commercial prospects for this technology seem brilliant. In particular, MspA conjugated with a polymerase (phi29) that steps the DNA through the pore has been used to decode long reads in which approximately 4 quadromers (4 nucleotides) affect the ion current of each level [32]. Reads of up to 4.5 kb in length were unambiguously aligned to a reference genome. Another nascent sequencing technology, MinION^{TM}, which uses an array of multiplexed proteinaceous nanopores, has been distributed to early access sites by Oxford Nanopore [33]. We have taken the opportunity to test an early access MinION instrument, which consists of an array of 2048 polymer membrane pores multiplexed to 512 read channels and embedded in a flow-cell. Protein pores are embedded in the membranes. Although the exact nature of the pores is proprietary, we have noted that not all the membranes are active (Fig. 3a). This is either due to a failure of pores to integrate due to the challenge of single pore insertion, or poor yield of proteinaceous pores surviving shipment and storage under current conditions. A DNA library is delivered through simple pipetting into an entry port on the MinION. The USB-stick sized instrument is connected to a computer, and events are base-called in the cloud using a proprietary algorithm, presumably similar to the Viterbi scheme outlined above.

The library is prepared by first shearing the DNA into ~8 kb fragments to increase the concentration of molecules. A higher molecular concentration will increase the throughput by minimizing the time pores stand empty; the probability of a pore capturing DNA is directly dependent on the concentration since capture is primarily a diffusive process, a property known as diffusion equivalent capacitance. The rate of capture, R, is given explicitly by: $R = 2\pi CDr$, where C denotes the concentration, r is the radius of capture and D is the diffusion equivalent capacitance [34], [35]. Ragged DNA ends generated by shearing are cleaned up using a standard end-polishing/dA-tailing kit. Next, adapters are ligated to the molecule: a hairpin on one side, and a single stranded leader on the other end that has a binding site for a ''motor'' protein. The library is incubated overnight with motor protein before addition to the instrument; this protein controls the translocation rate of DNA through the pore. For our library, we used λ-DNA, a relatively small (48.5kb) standard that is commercially available.

After loading the MinION, DNA molecules are captured by the pore, and driven through in a controlled fashion by the motor protein and electric field. Though the library is double stranded DNA, at first only the forward strand is fed through the pore. When the DNA reaches the hairpin adapter, the hairpin is unraveled and the reverse strand is then fed through the pore. This is similar to the SMRT bell adapter used in the Pacific Biosciences RS II [36], and provides error checking through independent sequencing of both the forward and reverse strand. With the current library preparation method, some of the strands will have hairpins on both ends, and some will have leaders on both ends. The dual-hairpins will not run, but the dual-leaders will, only providing a single strand read. Base-calling software can identify the hairpin location through an abasic site (DNA backbone without base) present in the hairpin. This is especially advantageous for a k-mer-based base-calling scheme; quadromers (as used by Oxford) that are difficult to call on the forward strand may be easy to call on the reverse strand, or vice versa. Current signatures are collected from individual reads and sent to a cloud-based base-caller: Metrichor^{TM}. We ran the device for 48 hrs periodically adding to the library to keep the molecular concentration high.

Using the Poretools package recently developed by Loman et al. [37] along with custom R-code, we analyzed the resulting data and extracted FASTQ files with sequence and base-quality information per base from each read of a lambda DNA sequence (Fig. 3). We extracted both raw reads and error-corrected reads (using the opposite strand) for comparison. Our run provided 228 Mb of raw sequencing data, with a max of 2.8 Mb from a single channel; 250 of the 512 channels provided data (Fig. 3a). Only 55.7Mb of this data has both forward and reverse reads with an accompanying higher base quality. This is likely due to failure of the hairpin to ligate to some of the library strands, as mentioned above. The read length shows an impressive 6 kb average for forward strand reads, 5.7 kb for reverse strand reads, and 7.3 kb for dual-strand error-corrected reads, though there are substantially less reverse and error-corrected reads (Fig 3b). The average base quality of the raw nanopore reads is relatively low (PHRED of 4.8; equivalent to an accuracy of 67 %), after employing error correction, the base quality increases to an accuracy of 88% (PHRED 9.2). For comparison, Illumina and Ion Torrent routinely report base-calling accuracy of 99.9% or greater (PHRED 30).

Typical sequence aligners, such as bowtie2 [38] and bwa [39] are optimized for alignment on hyper-accurate, short (<500 bp) read data, and would require significant optimization to align nanopore long reads. Instead, we used LAST [40] to align the nanopore reads to the reference lambda sequence. In this context, 72.3% (34,613 of 47,868) of the raw reads (both forward and reverse strand) aligned successfully and 94.1% (7225 of 7677) of the corrected reads, albeit with errors. There are three types of errors common in aligned

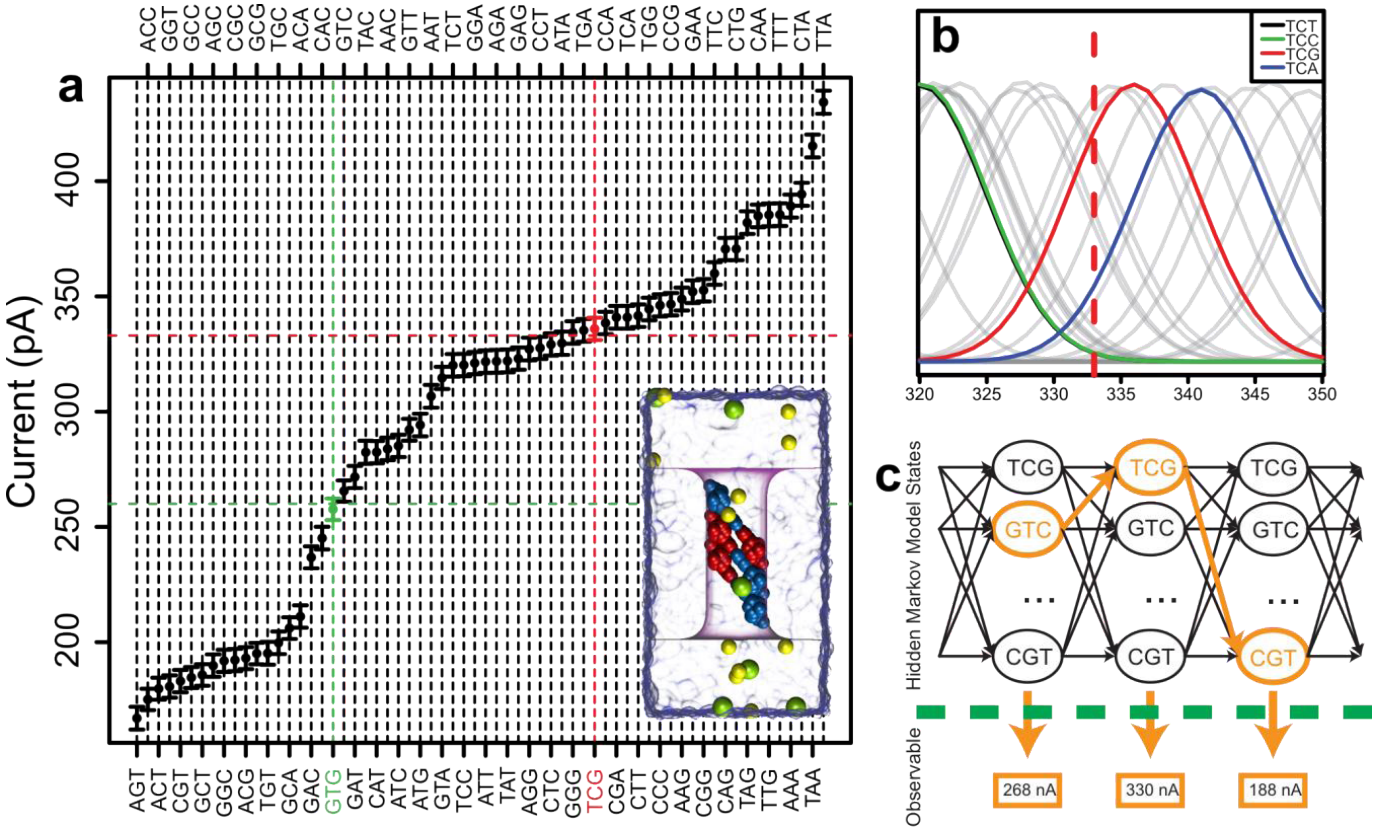

FIGURE 2. **Nanopore DNA Sequencing—base-calling. (a) Current values for all possible DNA triplets (4^3 =64) simulated using atomic resolution Brownian Dynamics, error bars indicate the expected standard deviation in ionic current (green dashed line) represents a typical current value for GTG triplet (green point), and red dashed line a typical current value for TCG triplet (red point). Inset: A simulated system for GCC. (b) Histograms of current values for a difficult to distinguish region: i.e. a current of 330pA is naively called as GGG, not as TCG. If we use the information from the previous triplet(in this case GTC), however, we can eliminate many of the possible triplet states as only states which share in common the last two bases of the last triplet (TC) as the first two bases of the new triplet are possible. The probability for each state is given as equal in this case (1/4). After convolving the probability of the states with the histograms, the calls become much easier. Unlikely states have been reduced to light gray. Note that TCC and TCT are still virtually indistinguishable from each other; if the current was 320pA, a third read would be needed to distinguish the bases. (c) The Viterbi algorithm operates on a state machine assumption. The operation of Viterbi's algorithm can be visualized by means of a trellis diagram; the Viterbi path is the path which maximizes the joint probabilities through the trellis, colored in orange. Adapted from reference [25].**

sequencing data: mismatches in which the base disagrees with the base in the reference; deletions in which the sequence data is missing bases present in the reference; or insertions in which the sequence data has bases not present in the reference. We would consider the insertions and deletions errors in event detection or translocation rate; and mismatches errors in the base-calling due to the low signal to noise.

We have plotted the fraction of aligned reads, for both the raw and error-corrected data, to show how many bases are correct, mismatched, inserted or deleted relative to a known λ reference genome. For the raw data, 48.7% of the bases were correct, 35.1% mismatched, 3.8% insertions and 16.2% deletions relative to the length of the aligned read. This demonstrates that both base-calling (mismatches) and translocation control are problematic. In particular, deletions could represent DNA slipping through the pore too rapidly. In contrast, after error correction, this improves to 67.4% of the bases correct, 24.2% mismatched, 7.5% insertions and 8.3% deletions relative to the length of the aligned read. As a different way of visualizing this data, we have used the Integrative Genomics Viewer (IGV) to plot the individual aligned reads (Fig. 3d). Mismatched bases are indicated by color, deletions by black lines and insertions by purple carets. Though the majority of the reads had many errors, the majority of the errors seem random rather than systematic. Only in a few locations are >20 % of the reads in disagreement with reference, as shown in the colored bars at the top. If we compute a consensus sequence at each position, we find only 7 errors in 48,502 bp; though it should be pointed out that we are using 1000× coverage of this small genome. It is likely that a more specific aligner may be needed to account for nanopore-style data that is optimized for the read length and common error types.

There is a niche market for long-read sequencing like this, which is satisfied by Pacific Biosciences SMRT sequencing right now. First, providing a scaffold for *de novo* sequencing to achieve long regions of contiguously assembled sequence (''contigs''). Typically, extremely deep coverage, i.e. an average of 100 reads covering each base, of short-read sequencing is needed, but an alternative is a scaffold of long reads with the short-reads providing accuracy and the long-reads providing position. A second application is the iden-

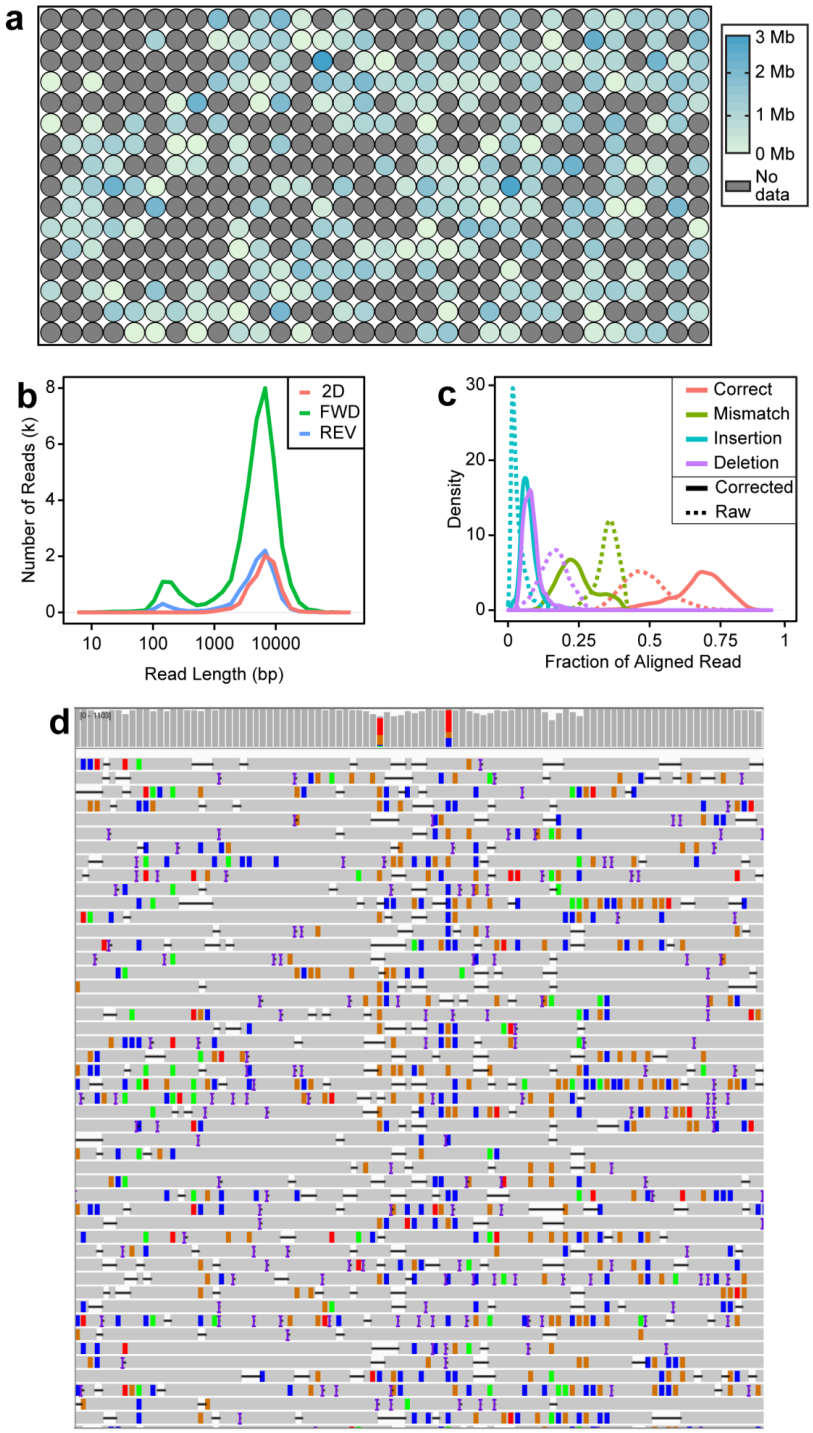

FIGURE 3. **Using the MinION to sequence DNA (a) Yield plot of DNA sequence produced per channel; each channel is represented by a circle. Channels in gray produced no data. Yield from other channels had a mean of 0.9 Mb and a standard deviation of 0.6 Mb with a max yield of 2.9 Mb. (b) Histogram of read length on log scale for forward strand (green), reverse strand (blue) and two-directional (error-corrected) reads. (c) Kernel smoothed density of base types from aligned reads plotting correct, mismatched, inserted or deleted bases versus the reference sequence. Both raw (dotted) and error-corrected (solid) fractions are plotted. (d) Results of data alignment plotted using IGV from 24001-24100 bp on the lambda genome. (top) Histogram shows coverage of the lambda genome (max of 1103×). Areas where more than 20% of the reads disagree with the reference λ genome are colored with the base distribution (A green; C blue; G orange, T red). Locations where less than 20 % of reads disagree are grey. (bottom) Each row represents an individual read, with agreements to the reference again plotted as grey rectangles, mismatches colored with the alternative base, insertions with a purple caret, and deletions as a thin black bar.**

tification of RNA splicing variants—short read sequencing can only provide information about individual exons or exon boundaries, but not the full isoforms of the RNA. The combination of exons could provide deeper information of altered expression. Finally, the long read sequencing can be critical to probe areas of repetitive sequence since aligning a short read

to those areas is difficult unless a unique region can be identified. Long reads can span repetitive regions to reach unique regions that facilitate alignment. Applying inexpensive and fast nanopore technology to DNA sequencing can facilitate not just genomics but also epigenomics (i.e. the methylation profile); [41] and transcriptomics (i.e., the sequence of the RNA).

B. DISCRIMINATING AND SEQUENCING PROTEINS

It is not enough to know just the genes to find a cure. Ever since the first draft of the human genome, [42], [43] there has been a new game in town with the potential for an even larger market: proteomics. The proteins expressed by genes represent the machinery of the cell—they make things work and are often the locus for disease. A protein is made up of a chain of amino acid (AA) residues. For example, human proteins as annotated in the NCBI database, range between 24–36,000 amino acids long, with a median of 469; the median molecular weight is 52.3 kD. Bacteria and archaea have similar, but slightly shorter average lengths [44]. Some proteins also contain disulfide bonds between cysteine residues that form cross-links between chains or parts of a chain. The three-dimensional architecture of the protein, which can be analyzed in terms of multiple folded components, determines its function [45]. The tertiary structure refers to the arrangement of AA residues separated from each other in the sequence, and to the pattern of disulfide bonds. The secondary structure refers to the spatial arrangement of proximate AA residues, some of which are periodic like the rod-like α helix and the β-sheet. For example, in an α-helix, which is only 500 pm in diameter, the AAs are spatially close together but on opposite sides, so that they are unlikely to contact each other. Finally, the primary structure of a protein is just the AA sequence; it largely dictates the 3D structure.

The first draft of the human proteome, [46], [47] the entire set of proteins expressed by the genome, [48] has just become available, which will doubtless advance medical research. This data was acquired with mass spectrometry (MS), the work-horse for protein identification [49], [50]. MS can sequence a protein of any size, but primarily relies on enzymatic digestion, which suffers from post-translational protein modification and, after digestion, it is difficult to assemble the sequence computationally as the size increases due to the large number of peptides. Furthermore, MS requires relatively concentrated samples (>fmole/L-scale) and can only analyze them one-at-a-time, limiting throughput. In contrast, the methods for analyzing nucleic acids rely on amplification via polymerase chain reaction (PCR) or sequencing-by-synthesis. However, both are unworkable for protein or other polymer analysis. Instead, the entire original molecule has to be sequenced. It is time for something completely different.

Both proteinaceous and solid-state nanopores can be effective tools for analysis of peptides and proteins [51]–[63]. The applications can be categorized in two ways: detection and quantitation of protein; and the discovery of protein primary and higher-order structure. In particular, α-HL has been used to detect protein structural features and even phosphorylation status of a protein, [58] whereas solid-state nanopores have been used to inform on the chemical, thermal, and electric field effects on protein folding [51], [55], [60] and protein-DNA interactions [61]–[63]. Protein levels may also be detected, either through labeling with a DNA aptamer [64] or through direct blockade measurement [60], [65]. One strategy employed for detection uses a nanopore as a stochastic sensor, relying on statistical inference from a compilation of distinctive current blockades. This scheme has already been thoroughly reviewed [57].

Recently, we tested the prospects for using a pore comparable in size to the tertiary structure of a protein as a stochastic sensor [60] to discriminate between two proteins bovine serum albumin (BSA, molecular weight 66.5 kDa with an approximate size of $14 \times 4 \times 4$ nm^3) [66] and streptavidin (STR, 52.8 kDa and a size of $6 \times 5 \times 5$ nm) [67]. To test the feasibility of discriminating between proteins, we tried to force STR and BSA through the same 7.4 nm pore, but could not detect any current transients associated with STR interacting with the pore. We attributed this observation to the relatively neutral charge on the STR protein: at pH 8, BSA supposedly has a charge of $-25e^-$, where e^- represents the elementary charge, whereas STR has a charge of only $-4e^-$, which is apparently insufficient to provide enough electric force to translocate it across the membrane through the pore. According to this interpretation, BSA can be discriminated by charge from STR perfectly at pH 8. The charge of the protein can be adjusted, however, by controlling the pH [68], [69]. A comparison of the ionic current blockade spaces associated with BSA at pH 8 and STR at pH 9.6, where the overall charge on the molecule is estimated to be $-12e^-$, reveals differences in the mean dwell time and percentage blockade (Fig. 4a).

To discriminate proteins using the pore as a stochastic sensor, each event should be classified by the distribution that defines it. In multivariate analysis, a common technique used to classify observations is linear discriminant analysis (LDA)—the dashed line in Figure 4a demarcates the spaces attributable to the two proteins. Correspondingly, the receiver operating characteristic (ROC) (Fig. 4a, inset) measures the ratio of true positives (an event that correctly identifies the protein) to false positives (an event that identifies the wrong protein) in the LDA model. The ROC specifies the probability to correctly identify BSA in a mixture, which is typically measured by the area under curve (AUC), as AUC=0.73. To this extent, it is also possible to discriminate two different conformations of the *same* protein using the same nanopore (Fig. 4b): one wild-type BSA and another denatured BSA. (BSA irreversibly denatures for temperatures >65° [68], [69]). We observed that the denatured BSA shows shallower blockades with a shorter duration. Thus, it is possible to discriminate between two different proteins (AUC=0.73) and even different conformations of the same protein (AUC=0.72). However, these classification schemes are imperfect due in part to the stochastic nature of the measurement.

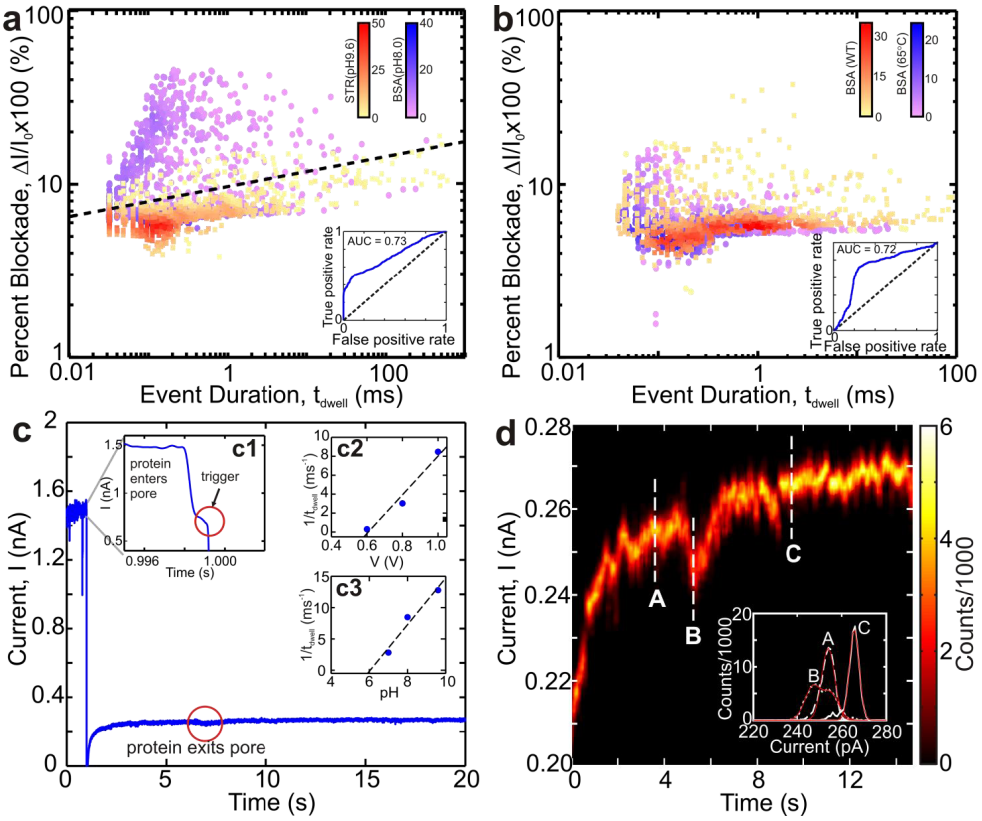

FIGURE 4. **Proteins translocating through a nanopore (a) Heat map of the percentage blockade current versus dwell time ($\Delta I/I_0$ *vs* t_{dwell}) for 1000 events of bovine serum albumin (BSA) at pH 8 (red circles) superimposed on a heat map of the same for streptavidin (STR) at pH 9.6 (blue squares) through the 7.4nm-diameter pore. The dashed black line demarcates the two groups of protein when the events are classified with an LDA. Inset: ROC of the protein discriminator with an AUC of 0.73. (b) Heat map of the percentage blockade current versus dwell time for 1000 events of wild-type BSA (WT) (red squares) and denatured BSA (blue circles) through the 4×11-nm pore. Inset: ROC with an AUC of 0.72. (c) A single protein trapped in a nanopore as evident in the current. When the protein enters the pore at V=0.6V, Inset (c1), it triggers a signal that switches the voltage bias to V=0.1V. After ~ 6 s the protein exits the pore. Inset (c2) shows the inverse dwell time versus bias voltage for BSA passing through a 5 × 5nm pore in 100 mM *KCl* at pH8. The linear fit to the data, indicated by the dashed line, extrapolates to a threshold of 0.59V. Inset (c3) shows the inverse dwell time versus pH of BSA in the same pore as (a2) at 1 V bias. (d) Intensity map showing current fluctuations within a moving 250 ms window associated with a trapped protein. Inset: Histograms of 1 s of current data at 3.6 (A), 5.25 (B) and 9.5 s (C) after the protein is trapped. Solid lines (red) are fits to the data. Adapted from reference [60].**

Instead of stochastic sensing on a large sample of proteins, we assert that it should be possible to detect and analyze a *single* protein trapped in a nanopore. Proteins inherently have a very specific distribution of surface charge, which is used to attract different targets to different parts of the protein. The exquisite control exercised over the electrostatic potential available in a nanometer-diameter pore could be exploited to identify the distinctive surface charge on a protein and trap it (Fig. 4c) [60]. The conditions required for trapping a protein in a pore can be inferred from the dependence of the reciprocal of the dwell time as a function of voltage and pH. The dwell time, $1/t_{dwell}$, vanishes below ~0.6 V or below pH 6 at 1V because no protein enters the pore without an electric force, and the force is determined by a combination of charge, which is affected by pH, and the electric field that is related to the applied voltage. Accordingly, BSA was forced into a pore smaller than the protein using 0.6 V at pH 8. When a dramatic change in the current is observed (see inset (c1)) corresponding to BSA entering the pore, it triggers a change in the bias from 0.6 V to 0.1 V resulting in a substantial reduction in the translocation velocity. The molecule eventually exits the pore after about 6 s. The compilation of intensity plots, produced by generating a histogram of the current in consecutive 250 ms windows, captures the amplitude of current fluctuations observed when the protein is trapped (Fig. 4d). Under these conditions, with the molecule trapped in the pore, the electric force is large enough to unfold the protein and the blockade current fluctuations presumably signal a change in the occluded volume in the pore. The Gaussian peak in the open pore current is represented in C (Fig. 4d, inset), while two different protein conformations are represented in A and B. Consequently, it was asserted that the fluctuations in the blockade current inform on the molecular configuration in the pore, reflecting a change in the occluded volume in the pore as the protein denatures or unfolds under force associated with the electric field [60].

Sequencing a protein will demand something more than this. Measurements of single polymers translocating through a nanopore are a promising prelude to sequencing a single molecule, [58], [70]–[72] but unlike DNA, the charge distribution along a protein is not uniform, so the translocation kinetics cannot be systematically controlled with the electric field in the pore. Alternative schemes rely more on diffusion to impel the protein after an attached DNA leader is forced through the pore by a field [58]. Another remedy used an enzymatic motor (ClpXP) to drive proteins progressively through αHL by repeatedly pulling on the substrate protein to unfold it [70].

Finally, whereas the single molecule sensitivity of a nanopore is incontrovertible, it has a drawback for detection of dilute concentrations of molecules that is related to the diffusion equivalent capacitance [34]. Regardless of whether the pore is biological or in a solid-state membrane, the majority of the electric field is focused in the central constriction so that a molecule must diffuse within a capture radius of the pore before the electric force impels it, which is only tens of nanometers in extent [34], [35]. Thus, the specifications for detecting a *single monomer* with a nanopore are very stringent—the geometry and electric field in the pore are determined by the size of the monomer and surface charge, while the capture rate increases only with proximity to the molecular source.

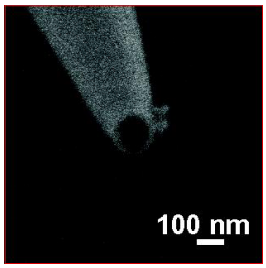

FIGURE 5. Nanopipettes for molecular imaging. A typical single barreled nanopipette.

C. NANOSCOPY: USING A NANOPORE FOR BIO-IMAGING

To improve the capture rate, a nanopipette can be used to move the pore closer to the molecular source. This configuration elicits a picture not unlike that of near field optical microscopy in which a pore aperture now collects a (molecular) flux (instead of light) to peer into biology on a nanoscale. Nanopipettes (Fig. 5) have already been used as nanometer-scale Coulter counters to detect everything from ions to proteins and DNA [73]–[86]. For example, a nanopipette can be used to perform scanning ion conductance microscopy (SICM) or even penetrate a living cell to provide a spatially-resolved chemical response [80]–[84]. In particular, it is possible to map the topography of a living cell using the ion current through the nanopipette, which decreases as the orifice approaches within a pore radius of the sample, by using a feedback signal to control the position of the probe [83]. Likewise, a nanopipette can be filled with an ionophore to form an ion selective electrode, which allows for spatially resolved sensing of the local ionic concentration [80]–[84]. Recent developments have included mapping the local surface charge with the ion current as a function of probe-surface distance at different biases, [84] and single cell nanobiopsy [85]. Thus, nanopipettes potentially offer a combination of single molecule precision with the spatial resolution of a scanning probe microscope.

Alternatively, instead of bringing the pore to the cell, the cell can be positioned immediately over a nanopore using optical tweezers [87], [88]. By doing so, the secretions from a single cell can be detected, classified [87] and even regulated [88]. However, since the concentration is so dilute, the secretome is easily contaminated by proteins found in the supernatant (e.g. from lysed cells), cell medium (e.g. BSA) or blood plasma. Moreover, due to the broad spectrum of molecular weight that comprises the secretome, a nanopore is prone to clogging [89].

D. PRECISELY TRANSFECTING A SINGLE CELL WITH A NANOPORE

We discovered serendipitously that by using the same electric field that impels a molecule through the pore, it is possible to transfect a cell by electroporation, provided it is in close proximity to the pore (Fig. 6) [88]. (In the supplement, video S2: transfection.wmv illustrates the use of a nanopore to transfect a single cell with fluorescent DNA via electroporation.) While our understanding is still incomplete, molecular dynamics simulations indicate that nanometer-scale biological pores (1–10 nm) can be formed in a cell membrane, driven by the runaway local electric field at the water-lipid interface [90]. The distribution of the electric field, due to the topography of the nanopore, is focused and confined to a region around the pore, allowing very low voltage transfection ($<$1 V) while, at the same time, making it unlikely to electroporate a cell anywhere else. However, to leverage the electric field outside the pore for electroporation, single cells must be positioned close to it. (Figs. 6a–c). This can be accomplished with high precision using optical tweezers [88].

To test the idea that a cell can be transfected with a nanopore, fluorescent DNA plasmids were impelled by the electric force associated with a 1V transmembrane bias (Fig. 6c). The fluorescence obtained from a confocal image of an MDA-MB-231 human breast cancer cell taken along an x-z slice, which includes the pore axis, illuminates the cell and the position of the synthetic pore (even though the membrane was hardly perceptible.) Thus, a cell in close proximity to the pore can be electroporated with 1 V. By controlling the duration of a voltage pulse and simultaneously measuring the pore current, a precise number of DNA molecules were delivered into the cell—serial transfections on the same cell are also possible this way. The correspondence between the blockades measured in the pore current (Fig. 6d) and the fluorescence associated with individual DNA plasmids (Fig. 6e) supports the contention that a cell can be transfected with single molecule accuracy. Below 50 molecules, the relative error

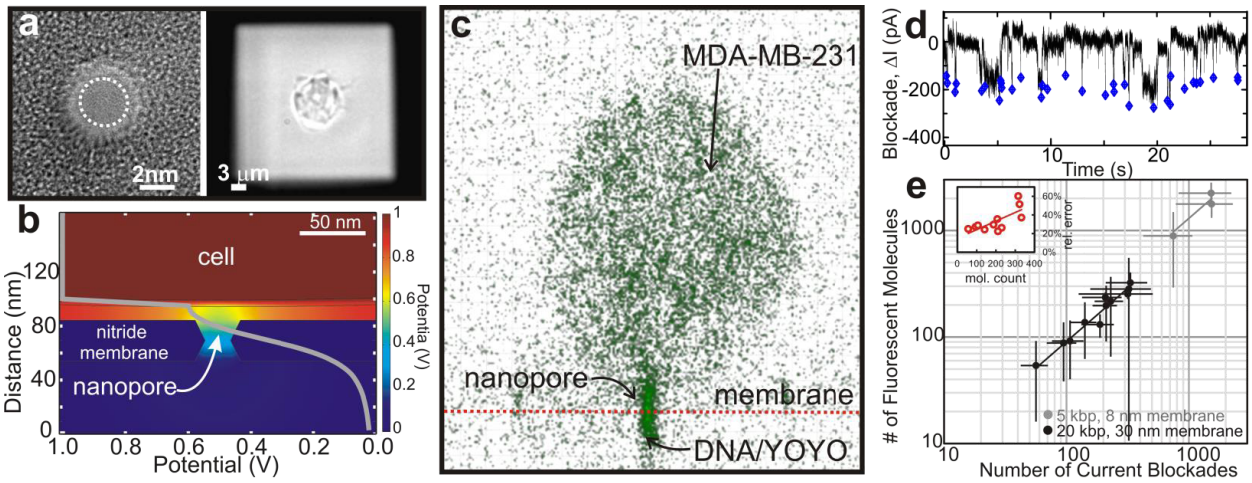

FIGURE 6. **Using a nanopore to transfect mammalian cells via electroporation with molecular precision. (a, left) Transmission electron micrograph (TEM) of a 2.5 nm diameter nanopore in a 30 nm thick Si_3N_4 membrane. (a, right) Top-down optical micrograph of a cell positioned over a nanopore in a 30 nm thick Si_3N_4 membrane 35 μm on edge. (b) Finite element simulation of the cell-synthetic nanopore interface showing the electric potential in the vicinity of a cell 10 nm above the silicon nitride membrane. (c) A confocal (x-z) slice showing the accumulation of 7 kbp YOYO-1 intercalated circular plasmids in an MDA-MB-231 cell positioned over a 20.5 nm diameter pore. The fluorescence associated with individual molecules of dsDNA shows the outline of the cell. The nitride membrane (indicated by the dashed red line) is hardly perceptible, but the fluorescent DNA in the nanopore is easily visualized. (d) Measurement of the pore current during transfection. Blockades that appear in the current indicate the translocation of a single dsDNA molecule across the silicon nitride membrane through the nanopore. Events attributed to the translocation of one DNA are marked with blue diamonds. (e) The correspondence between events counted using the blockade current and the resulting fluorescence from accumulated YOYO-1 intercalated in DNA in 14 transfected cells. Cells were transfected with 56-1534 molecules. Inset: The relative error in the molecular count using the blockade current. Adapted from reference [88].**

associated with the fluorescence measurement precludes an accurate count; however, the blockade count can be extended to single molecule sensitivity (Fig. 6e, inset).

Subsequently, the capability to transfect cells with nucleic acids and reprogram their functionality by gene induction and silencing, while maintaining viability, was established unequivocally [88]. Synthetic biology demands tools like this capable of precisely modifying a cell's genetic code and modulating gene expression to create a predictable phenotype. To gain control of the cell and produce a predictable function, critical points in that network need to be regulated [91]. In particular, the transcription factors that dictate cell fate are translated from less than one thousand transcripts in a cell [92]. Therefore, a method like this which uses a nanopore for conveying a biologically relevant number of distinct bio-molecules into a cell is required. Finally, from another perspective, a cell can be likened to a chemical micro-reactor comprised from organelles and nanochannels (i.e. mitochondria, Golgi apparatus, etc.) that act like nano-reactors. Nanometer- and micrometer-scale reactors can produce highly efficient, selective reactions with high yield because mass transport limitations are practically eliminated by confining the reactions to sub-femtoliter volumes where diffusion occurs rapidly [93], [94]. Thus, a nanopore can be utilized to produce highly efficient "perfect" reactions.

III. CONCLUSION

In conclusion, the future is brilliant, if you think small and do a bit more research.

Nanopores can be used to both READ: detect and sequence DNA and sense proteins, and WRITE DNA into cells. These tools will provide methods to explore areas of biology either impractical to reach, or at least logistically intractable. It places single-molecule DNA, and possibly, eventually protein sequencing, within the reach of researchers or clinical labs, no longer reserved to genomics or mass spectrometry specialists. However, nagging problems associated with chemical specificity, imprecise manufacturing, the imperfect control of a translocation, and the transport of a single molecule to the pore could stand improvement. Prospects for synthetic biology (and manufacturing) using nanopores to program cells (or micelles) and deliver materials are especially alluring. Chemical processing generally becomes more efficient in a microreactor because mass transport limitations are practically eliminated. However, the synthesis, so far, has been focused at a single cell or few nano-reactor level; it needs to be scaled up.

REFERENCES

[1] C. W. H, "Means for counting particles suspended in a fluid," U.S. 2 656 508, Oct. 20, 1953.
[2] K. K. Likharev, "Single-electron devices and their applications," *Proc. IEEE*, vol. 87, no. 4, pp. 606–632, Apr. 1999.
[3] G. Church, D. W. Deamer, D. Branton, R. Baldarelli, and J. Kasianowicz, "Measuring physical properties," U.S. Patent 5 795 782, Aug. 18, 1998.
[4] J. J. Kasianowicz, E. Brandin, D. Branton, and D. W. Deamer, "Characterization of individual polynucleotide molecules using a membrane channel," *Proc. Nat. Acad. Sci. United States Amer.*, vol. 93, no. 24, pp. 13770–13773, Nov. 1996.
[5] S. Lutz, "Beyond directed evolution–semi-rational protein engineering and design," *Current Opinion Biotechnol.*, vol. 21, no. 6, pp. 734–743, Dec. 2010.
[6] D. Branton *et al.*, "The potential and challenges of nanopore sequencing," *Nature Biotechnol.*, vol. 26, pp. 1146–1153, Oct. 2008.
[7] W. Timp, U. M. Mirsaidov, D. Wang, J. Comer, A. Aksimentiev, and G. Timp, "Nanopore sequencing: Electrical measurements of the code of life," *IEEE Trans. Nanotechnol.*, vol. 9, no. 3, pp. 281–294, May 2010.

[8] B. M. Venkatesan and R. Bashir, "Nanopore sensors for nucleic acid analysis," *Nature Nanotechnol.*, vol. 6, no. 10, pp. 615–624, Sep. 2011.
[9] E. R. Mardis, "The impact of next-generation sequencing technology on genetics," *Trends Genet.*, vol. 24, no. 3, pp. 133–141, 2008.
[10] M. Pop and S. L. Salzberg, "Bioinformatics challenges of new sequencing technology," *Trends Genet.*, vol. 24, no. 3, pp. 142–149, Mar. 2008.
[11] S. Koren *et al.*, "Hybrid error correction and *de novo* assembly of single-molecule sequencing reads," *Nature Biotechnol.*, vol. 30, no. 7, pp. 693–700, Jul. 2012.
[12] G. Sigalov, J. Comer, G. Timp, and A. Aksimentiev, "Detection of DNA sequences using an alternating electric field in a nanopore capacitor," *Nano Lett.*, vol. 8, no. 1, pp. 56–63, 2008.
[13] L.-H. Yeh, M. Zhang, S. W. Joo, and S. Qian, "Slowing down DNA translocation through a nanopore by lowering fluid temperature," *Electrophoresis*, vol. 33, no. 23, pp. 3458–3465, Dec. 2012.
[14] D. Fologea, J. Uplinger, B. Thomas, D. S. McNabb, and J. Li, "Slowing DNA translocation in a solid-state nanopore," *Nano Lett.*, vol. 5, no. 9, pp. 1734–1737, Sep. 2005.
[15] G. M. Cherf, K. R. Lieberman, H. Rashid, C. E. Lam, K. Karplus, and M. Akeson, "Automated forward and reverse ratcheting of DNA in a nanopore at 5-Å precision," *Nature Biotechnol.*, vol. 30, no. 4, pp. 344–348, 2012.
[16] E. A. Manrao *et al.*, "Reading DNA at single-nucleotide resolution with a mutant MspA nanopore and phi29 DNA polymerase," *Nature Biotechnol.*, vol. 30, pp. 349–353, Mar. 2012.
[17] U. Mirsaidov, J. Comer, V. Dimitrov, A. Aksimentiev, and G. Timp, "Slowing the translocation of double-stranded DNA using a nanopore smaller than the double helix," *Nanotechnology*, vol. 21, no. 39, p. 395501, Oct. 2010.
[18] B. Luan, H. Peng, S. Polonsky, S. Rossnagel, G. Stolovitzky, and G. Martyna, "Base-by-base ratcheting of single stranded DNA through a solid-state nanopore," *Phys. Rev. Lett.*, vol. 104, no. 23, p. 238103, Jun. 2010.
[19] E. M. Nelson, H. Li, and G. Timp, "Direct, concurrent measurements of the forces and currents affecting DNA in a nanopore with comparable topography," *ACS Nano*, vol. 8, no. 6, pp. 5484–5493, 2014.
[20] C. Ho *et al.*, "Electrolytic transport through a synthetic nanometer-diameter pore," *Proc. Nat. Acad. Sci. United States Amer.*, vol. 102, no. 30, pp. 10445–10450, 2005.
[21] C. Hyun, H. Kaur, R. Rollings, M. Xiao, and J. Li, "Threading immobilized DNA molecules through a solid-state nanopore at >100 μs per base rate," *ACS Nano*, vol. 7, no. 7, pp. 5892–5900, Jun. 2013.
[22] U. F. Keyser *et al.*, "Direct force measurements on DNA in a solid-state nanopore," *Nature Phys.*, vol. 2, no. 7, pp. 473–477, 2006.
[23] G. M. King and J. A. Golovchenko, "Probing nanotube-nanopore interactions," *Phys. Rev. Lett.*, vol. 95, no. 21, p. 216103, Nov. 2005.
[24] W. J. Bruno, G. Ullah, D.-O. D. Mak, and J. E. Pearson, "Automated maximum likelihood separation of signal from baseline in noisy quantal data," *Biophys. J.*, vol. 105, no. 1, pp. 68–79, 2013.
[25] W. Timp, J. Comer, and A. Aksimentiev, "DNA base-calling from a nanopore using a Viterbi algorithm," *Biophys. J.*, vol. 102, no. 10, pp. L37–L39, 2012.
[26] D. Stoddart, G. Maglia, E. Mikhailova, A. J. Heron, and H. Bayley, "Multiple base-recognition sites in a biological nanopore: Two heads are better than one," *Angew. Chem. Int. Ed.*, vol. 49, no. 3, pp. 556–559, 2010.
[27] S. Garaj, S. Liu, J. A. Golovchenko, and D. Branton, "Molecule-hugging graphene nanopores," *Proc. Nat. Acad. Sci. United States Amer.*, vol. 110, no. 30, pp. 12192–12196, Jul. 2013.
[28] A. B. Farimani, K. Min, and N. R. Aluru, "DNA base detection using a single-layer MoS_2," *ACS Nano*, vol. 8, no. 8, pp. 7914–7922, Aug. 2014.
[29] G. F. Schneider *et al.*, "Tailoring the hydrophobicity of graphene for its use as nanopores for DNA translocation," *Nature Commun.*, vol. 4, p. 2619, Oct. 2013.
[30] S. Huang *et al.*, "Identifying single bases in a DNA oligomer with electron tunnelling," *Nature Nanotechnol.*, vol. 5, pp. 868–873, Nov. 2010.
[31] Z. S. Siwy and S. Howorka, "Engineered voltage-responsive nanopores," *Chem. Soc. Rev.*, vol. 39, no. 3, pp. 1115–1132, 2009.
[32] A. H. Laszlo *et al.*, "Decoding long nanopore sequencing reads of natural DNA," *Nature Biotechnol.*, vol. 32, no. 8, pp. 829–834, Jun. 2014.
[33] *Oxford Nanopore Home Page*. [Online]. Available: http://www.nanoporetech.com/, accessed Oct. 2014
[34] P. R. Nair and M. A. Alam, "Performance limits of nanobiosensors," *Appl. Phys. Lett.*, vol. 88, no. 23, p. 233120, 2006.
[35] J. Nakane, M. Akeson, and A. Marziali, "Evaluation of nanopores as candidates for electronic analyte detection," *Electrophoresis*, vol. 23, no. 16, pp. 2592–2601, Aug. 2002.
[36] K. J. Travers, C.-S. Chin, D. R. Rank, J. S. Eid, and S. W. Turner, "A flexible and efficient template format for circular consensus sequencing and SNP detection," *Nucl. Acids Res.*, vol. 38, no. 15, p. e159, Aug. 2010.
[37] N. J. Loman and A. R. Quinlan, "Poretools: A toolkit for analyzing nanopore sequence data," *Bioinformatics*, p. btu555, Aug. 2014.
[38] B. Langmead and S. L. Salzberg, "Fast gapped-read alignment with Bowtie 2," *Nature Methods*, vol. 9, no. 4, pp. 357–359, Apr. 2012.
[39] H. Li and R. Durbin, "Fast and accurate short read alignment with Burrows–Wheeler transform," *Bioinformatics*, vol. 25, no. 14, pp. 1754–1760, Jul. 2009.
[40] S. M. Kiełbasa, R. Wan, K. Sato, P. Horton, and M. C. Frith, "Adaptive seeds tame genomic sequence comparison," *Genome Res.*, vol. 21, no. 3, pp. 487–493, Mar. 2011.
[41] P. A. Callinan and A. P. Feinberg, "The emerging science of epigenomics," *Human Molecular Genet.*, vol. 15, pp. R95–R101, Apr. 2006.
[42] E. S. Lander *et al.*, "Initial sequencing and analysis of the human genome," *Nature*, vol. 409, no. 6822, pp. 860–921, 2001.
[43] J. C. Venter *et al.*, "The sequence of the human genome," *Science*, vol. 291, no. 5507, pp. 1304–1351, 2001.
[44] L. Brocchieri and S. Karlin, "Protein length in eukaryotic and prokaryotic proteomes," *Nucl. Acids Res.*, vol. 33, no. 10, pp. 3390–3400, 2005.
[45] L. Stryer, *Biochemistry*. New York, NY, USA: Freeman, 1999.
[46] M. Wilhelm *et al.*, "Mass-spectrometry-based draft of the human proteome," *Nature*, vol. 509, pp. 582–587, May 2014.
[47] M.-S. Kim *et al.*, "A draft map of the human proteome," *Nature*, vol. 509, no. 7502, pp. 575–581, May 2014.
[48] The ENCODE Project Consortium, "An integrated encyclopedia of DNA elements in the human genome," *Nature*, vol. 489, no. 7414, pp. 57–74, 2012.
[49] A. F. M. Altelaar, J. Munoz, and A. J. R. Heck, "Next-generation proteomics: Towards an integrative view of proteome dynamics," *Nature Rev. Genet.*, vol. 14, no. 1, pp. 35–48, 2013.
[50] B. F. Cravatt, G. M. Simon, and J. R. Yates, III, "The biological impact of mass-spectrometry-based proteomics," *Nature*, vol. 450, pp. 991–1000, Dec. 2007.
[51] D. S. Talaga and J. Li, "Single-molecule protein unfolding in solid state nanopores," *J. Amer. Chem. Soc.*, vol. 131, no. 26, pp. 9287–9297, 2009.
[52] E. C. Yusko *et al.*, "Controlling protein translocation through nanopores with bio-inspired fluid walls," *Nature Nanotechnol.*, vol. 6, pp. 253–260, Feb. 2011.
[53] R. Wei, V. Gatterdam, R. Wieneke, R. Tampé, and U. Rant, "Stochastic sensing of proteins with receptor-modified solid-state nanopores," *Nature Nanotechnol.*, vol. 7, pp. 257–263, Mar. 2012.
[54] B. Cressiot *et al.*, "Protein transport through a narrow solid-state nanopore at high voltage: Experiments and theory," *ACS Nano*, vol. 6, no. 7, pp. 6236–6243, 2012.
[55] K. J. Freedman *et al.*, "Chemical, thermal, and electric field induced unfolding of single protein molecules studied using nanopores," *Anal. Chem.*, vol. 83, no. 13, pp. 5137–5144, May 2011.
[56] D. Fologea, B. Ledden, D. S. McNabb, and J. Li, "Electrical characterization of protein molecules by a solid-state nanopore," *Appl. Phys. Lett.*, vol. 91, no. 5, p. 053901, Jul. 2007.
[57] L. Movileanu, "Interrogating single proteins through nanopores: Challenges and opportunities," *Trends Biotechnol.*, vol. 27, no. 6, pp. 333–341, Jun. 2009.
[58] C. B. Rosen, D. Rodriguez-Larrea, and H. Bayley, "Single-molecule site-specific detection of protein phosphorylation with a nanopore," *Nature Biotechnol.*, vol. 32, no. 2, pp. 179–181, Jan. 2014.
[59] J. Li, D. Fologea, R. Rollings, and B. Ledden, "Characterization of protein unfolding with solid-state nanopores," *Protein Peptide Lett.*, vol. 21, no. 3, pp. 256–265, Mar. 2014.
[60] E. M. Nelson, V. Kurz, J. Shim, W. Timp, and G. Timp, "Using a nanopore for single molecule detection and single cell transfection," *Analyst*, vol. 137, no. 13, pp. 3020–3027, Jul. 2012.
[61] Q. Zhao *et al.*, "Detecting SNPs using a synthetic nanopore," *Nano Lett.*, vol. 7, no. 6, pp. 1680–1685, 2007.
[62] B. Dorvel *et al.*, "Analyzing the forces binding a restriction endonuclease to DNA using a synthetic nanopore," *Nucl. Acids Res.*, vol. 37, no. 12, pp. 4170–4179, Jul. 2009.
[63] J. Shim *et al.*, "Detection and quantification of methylation in DNA using solid-state nanopores," *Sci. Rep.*, vol. 3, p. 1389, Mar. 2013.

[64] D. J. Niedzwiecki, R. Iyer, P. N. Borer, and L. Movileanu, "Sampling a biomarker of the human immunodeficiency virus across a synthetic nanopore," *ACS Nano*, vol. 7, no. 4, pp. 3341–3350, Apr. 2013.
[65] D. J. Niedzwiecki, J. Grazul, and L. Movileanu, "Single-molecule observation of protein adsorption onto an inorganic surface," *J. Amer. Chem. Soc.*, vol. 132, no. 31, pp. 10816–10822, Aug. 2010.
[66] A. K. Wright and M. R. Thompson, "Hydrodynamic structure of bovine serum albumin determined by transient electric birefringence," *Biophys. J.*, vol. 15, no. 2, pp. 137–141, Feb. 1975.
[67] I. L. Trong, Z. Wang, D. E. Hyre, T. P. Lybrand, P. S. Stayton, and R. E. Stenkamp, "Streptavidin and its biotin complex at atomic resolution," *Acta Crystallograph. Sec. D, Biol. Crystallogr.*, vol. 67, no. 9, pp. 813–821, Sep. 2011.
[68] R. Wetzel *et al.*, "Temperature behaviour of human serum albumin," *Eur. J. Biochem.*, vol. 104, no. 2, pp. 469–478, 1980.
[69] A. Das, R. Chitra, R. R. Choudhury, and M. Ramanadham, "Structural changes during the unfolding of Bovine serum albumin in the presence of urea: A small-angle neutron scattering study," *Pramana*, vol. 63, no. 2, pp. 363–368, 2004.
[70] J. Nivala, D. B. Marks, and M. Akeson, "Unfoldase-mediated protein translocation through an α-hemolysin nanopore," *Nature Biotechnol.*, vol. 31, no. 3, pp. 247–250, Mar. 2013.
[71] D. Rodriguez-Larrea and H. Bayley, "Multistep protein unfolding during nanopore translocation," *Nature Nanotechnol.*, vol. 8, pp. 288–295, Mar. 2013.
[72] C. Merstorf *et al.*, "Wild type, mutant protein unfolding and phase transition detected by single-nanopore recording," *ACS Chem. Biol.*, vol. 7, no. 4, pp. 652–658, 2012.
[73] C. A. Morris, A. K. Friedman, and L. A. Baker, "Applications of nanopipettes in the analytical sciences," *Analyst*, vol. 135, no. 9, pp. 2190–2202, 2010.
[74] W. Li *et al.*, "Single protein molecule detection by glass nanopores," *ACS Nano*, vol. 7, no. 5, pp. 4129–4134, 2013.
[75] B. Zhang, M. Wood, and H. A. Lee, "A silica nanochannel and its applications in sensing and molecular transport," *Anal. Chem.*, vol. 81, no. 13, pp. 5541–5548, 2009.
[76] N. Ebejer, A. G. Güell, S. C. S. Lai, K. McKelvey, M. E. Snowden, and P. R. Unwin, "Scanning electrochemical cell microscopy: A versatile technique for nanoscale electrochemistry and functional imaging," *Annu. Rev. Anal. Chem.*, vol. 6, pp. 329–351, Jun. 2013.
[77] B. R. Horrocks, M. V. Mirkin, D. T. Pierce, A. J. Bard, G. Nagy, and K. Toth, "Scanning electrochemical microscopy. 19. Ion-selective potentiometric microscopy," *Anal. Chem.*, vol. 65, no. 9, pp. 1213–1224, 1993.
[78] H. S. White and A. Bund, "Ion current rectification at nanopores in glass membranes," *Langmuir*, vol. 24, no. 5, pp. 2212–2218, 2008.
[79] S. Umehara, M. Karhanek, R. W. Davis, and N. Pourmand, "Label-free biosensing with functionalized nanopipette probes," *Proc. Nat. Acad. Sci. United States Amer.*, vol. 106, no. 12, pp. 4611–4616, 2009.
[80] P. K. Hansma, B. Drake, O. Marti, S. A. Gould, and C. B. Prater, "The scanning ion-conductance microscope," *Science*, vol. 243, no. 4891, pp. 641–643, 1989.
[81] L. J. Steinbock, O. Otto, C. Chimerel, J. Gornall, and U. F. Keyser, "Detecting DNA folding with nanocapillaries," *Nano Lett.*, vol. 10, no. 7, pp. 2493–2497, 2010.
[82] B. Vilozny, P. Actis, R. A. Seger, and N. Pourmand, "Dynamic control of nanoprecipitation in a nanopipette," *ACS Nano*, vol. 5, no. 4, pp. 3191–3197, 2011.
[83] J. Rheinlaender, N. A. Geisse, R. Proksch, and T. E. Schäffer, "Comparison of scanning ion conductance microscopy with atomic force microscopy for cell imaging," *Langmuir*, vol. 27, no. 2, pp. 697–704, 2011.
[84] K. McKelvey, S. L. Kinnear, D. Perry, D. Momotenko, and P. R. Unwin, "Surface charge mapping with scanning ion conductance microscopy," *J. Amer. Chem. Soc.*, vol. 36, no. 39, pp. 13735–13744, Sep. 2014.
[85] P. Actis *et al.*, "Compartmental genomics in living cells revealed by single-cell nanobiopsy," *ACS Nano*, vol. 8, no. 1, pp. 546–553, 2014.
[86] P. Novak *et al.*, "Nanoscale live-cell imaging using hopping probe ion conductance microscopy," *Nature Methods*, vol. 6, pp. 279–281, Mar. 2009.
[87] V. Kurz, T. Tanaka, K. McKelvey, E. Nelson, and G. Timp, "Single cell secretomics: Detecting secretions from single cancer cells," unpublished.
[88] V. Kurz, T. Tanaka, and G. Timp, "Single cell transfection with single molecule resolution using a synthetic nanopore," *Nano Lett.*, vol. 14, no. 2, pp. 604–611, 2014.
[89] V. Kurz, E. M. Nelson, J. Shim, and G. Timp, "Direct visualization of single-molecule translocations through synthetic nanopores comparable in size to a molecule," *ACS Nano*, vol. 7, no. 5, pp. 4057–4069, 2013.
[90] D. P. Tieleman, "The molecular basis of electroporation," *BMC Biochem.*, vol. 5, no. 1, p. 10, Jul. 2004.
[91] Y.-Y. Liu, J.-J. Slotine, and A.-L. Barabási, "Controllability of complex networks," *Nature*, vol. 473, pp. 167–173, May 2011.
[92] J. M. Vaquerizas, S. K. Kummerfeld, S. A. Teichmann, and N. M. Luscombe, "A census of human transcription factors: Function, expression and evolution," *Nature Rev. Genet.*, vol. 10, no. 4, pp. 252–263, Apr. 2009.
[93] J. M. Thomas and R. Raja, "Nanopore and nanoparticle catalysts," *Chem. Rec.*, vol. 1, no. 6, pp. 448–466, 2001.
[94] C. Ma, N. M. Contento, L. R. Gibson, II, and P. W. Bohn, "Redox cycling in nanoscale-recessed ring-disk electrode arrays for enhanced electrochemical sensitivity," *ACS Nano*, vol. 7, no. 6, pp. 5483–5490, 2013.

WINSTON TIMP (M'06) received the Ph.D. degree in electrical engineering from the Massachusetts Institute of Technology, Cambridge, MA, USA, in 2007, working under P. Matsudaira the Whitehead Institute of Biomedical Research. He subsequently worked as a Post-Doctoral Fellow at the Johns Hopkins School of Medicine, Baltimore, MD, USA, with Andrew Feinberg and Andre Levchenko. He joined the Biomedical Engineering Faculty at Johns Hopkins University, in 2013, as an Assistant Professor. His laboratory is focused on two main areas—dissecting how epigenetics operates on the single cell level and parsing the biophysical mechanisms of epigenetics on a single molecule basis. He is creating new tools to explore these questions using a combination of molecular biology, microscopy, next-generation sequencing, and nanotechnology.

Using these tools, he will gain a better understanding of the interaction between the microenvironment and epigenetics—giving a better idea, using an *in vitro*, controllable model, of how epigenetic changes identified in clinical samples are actually affecting cellular behavior. These tools will also give a greater understanding of the mechanisms of epigenetics on the biophysical level, allowing for the development of targeted therapies, to decode the meaning of the epigenetic patterns.

ALLISON M. NICE received the bachelor's degree in biology from the University of California at Santa Cruz, Santa Cruz, CA, USA, in 2012. She then worked for a year in cell culture development at Genentech, INC., South San Francisco, CA, USA. She is currently a Laboratory Techician with the Timp Laboratory, Johns Hopkins University, Baltimore, MD, USA, and is currently pursuing the master's degree in biotechnology.

EDWARD M. NELSON received the B.A. degree in physics from Hamilton College, Clinton, NY, USA, in 2001, and the Ph.D. degree in physics from the University of Rochester, Rochester, NY, USA, in 2009, working under the supervision of L. J. Rothberg, where he studied biomolecule/nanoparticle interactions. He is currently a Post-Doctoral Research Associate with the Department of Electrical Engineering, University of Notre Dame, Notre Dame, IN, USA. His primary research focus is to investigate the interaction between biological molecules, such as DNA and proteins, and synthetic materials using single molecule atomic force spectroscopy, optical tweezers, and electron microscopy, in order to understand the limitations of next generation sequencing technology.

VOLKER KURZ received the M.S. degree in physics from the State University of New York at Buffalo, Buffalo, NY, USA, in 2007, and the Ph.D. degree in physics from the University of Heidelberg, Heidelberg, Germany, in 2011, working under the supervision of Prof. M. Grunze and P. Koelsch investigating properties of various polymers at the water/polymer interface using nonlinear optical spectroscopy. Applying sum-frequency generating spectroscopy, he determined molecular orientations and made conclusions about entropy at interfaces to learn about the interaction of water with polymer films. He is currently a Post-Doctoral Fellow with the University of Notre Dame, Notre Dame, IN, USA, working under the supervision of Prof. G. Timp. His research interests include biophysics, nanopores, and optics. He is currently focused on both tissue engineering using live-cell lithography and also developing new tools for biology based on synthetic nanopores. With a synthetic nanopore, he electroporated single cells with single molecule precision achieving high efficiency and further analyzed the spectrum of single molecules secreted by cells in terms of their capability of blocking the electrolytic current through a nanopore.

KIM McKELVEY received the B.A.Sc. and master's degrees in computational modeling from the University of Otago, Dunedin, New Zealand, in 2005 and 2006, respectively, the master's degree in mathematical biology and biophysical chemistry from the University of Warwick, Coventry, U.K., in 2009, after time in the computer games industry, and the Ph.D. degree from the University of Warwick, in 2012, with Prof. Unwin, with a focus on new methods that improved the resolution and functionality of electrochemical scanning probe microscopy, and applications to biophysical problems. He is currently a Post-Doctoral Fellow with the University of Notre Dame, Notre Dame, IN, USA, with Prof. Timp.

GREGORY TIMP (M'94–F'07) received the Ph.D. degree in electrical engineering from the Massachusetts Institute of Technology, Cambridge, MA, USA, in 1984, under the supervision of M. Dresselhaus. From 1984 to 1986, he was a Post-Doctoral Fellow in Low-Temperature Transport and Nanostructure Physics with the IBM Thomas J. Watson Research Center, Yorktown Heights, NY, USA, with A. Fowler. In 1986, he joined Bell Labs, Murray Hill, NJ, USA, where he was involved in the research on nanostructure physics.

As a part of collaboration, he investigated low-temperature transport in electron waveguides and high-mobility nanostructures, which was so short that the transport is ballistic. In another effort, he explored the use of optical traps and laser focusing on single atoms for lithography applications. From 2000 to 2009, he was a member of the Department of Electrical and Computer Engineering and the Beckman Institute for Advanced Science and Technology at the University of Illinois at Urbana-Champaign, Champaign, IL, USA. He is currently the Keough-Hesburgh Professor of Electrical Engineering and Biological Sciences with the University of Notre Dame, Notre Dame, IN, USA, where he has been involved in research on the boundary between biology and nanoelectronics. His research interests include using nanopore sensors to detect the electronic structure of biomolecules and using optical tweezers to manipulate nanoparticles and living cells into large arrays, and super high frequency >30-GHz circuit design using radio frequency MOSFETs.

Prof. Timp has authored over 100 articles in refereed journals, given over 100 invited and plenary seminars, co-authored several books on nanotechnology, and holds several patents. He is a fellow of the American Association for the Advancement of Science and the American Physical Society. He is a fellow and founding member of the American Academy of Nanomedicine, and a member of the American Biophysical Society, the American Vacuum Society, and the Electrochemical Society.